https://doi.org/10.5194/tc-2020-235
Preprint. Discussion started: 21 September 2020

The Cryosphere Discussions
Open Access
EGU

The transferability of adjoint inversion products between different ice flow models

Jowan M. Barnes[1], Thiago Dias dos Santos[2,3], Daniel Goldberg[4], G. Hilmar Gudmundsson[1], Mathieu Morlighem[2], and Jan De Rydt[1]

[1]Department of Geography and Environmental Sciences, Northumbria University, Newcastle upon Tyne, UK
[2]Department of Earth System Science, University of California, Irvine, CA, USA
[3]Centro Polar e Climático, Universidade Federal do Rio Grande do Sul, Porto Alegre, RS, Brazil
[4]School of GeoSciences, University of Edinburgh, Edinburgh, UK

Correspondence: Jowan M. Barnes (jowan.barnes@northumbria.ac.uk)

Abstract. Among the most important challenges faced by ice flow models is how to represent basal and rheological conditions, which are challenging to obtain from direct observations. A common practice is to use numerical inversions to calculate estimates for the unknown properties, but there are many possible methods and not one standardised approach. As such, every ice flow model has a unique initialisation procedure. Here we compare the outputs of inversions from three different ice flow models, each employing a variant of adjoint-based optimisation to calculate basal sliding coefficients and flow rate factors using the same observed surface velocities and ice thickness distribution. The region we focus on is the Amundsen Sea Embayment in West Antarctica, the subject of much investigation due to rapid changes in the area over recent decades. We find that our inversions produce similar distributions of basal sliding across all models, despite using different techniques, implying that the methods used are highly robust and represent the physics without much influence by individual model behaviours. Transferring the products of inversions between models results in time-dependent simulations displaying variability on the order of or lower than existing model intercomparisons and process studies. While the successful transfer of inversion outputs from one model to another requires some extra effort and technical knowledge of the particular models involved, it is certainly possible and could indeed be useful for future intercomparison projects.

1 Introduction

Many ice flow models use inverse methods to calculate initial conditions for properties of the ice for which directly observed data do not exist, or are of poor quality. Inversion is an iterative process which starts from an initial guess, called a prior, and obtains improved values for the unknown property based on its relationship to a well-observed property such as surface velocity. This process is generally undertaken for at least one of ice rheology (flow rate factor, A), basal sliding and bed topography. The use of such methods in glaciology dates back to MacAyeal (1992), who used control methods to derive a distribution of

https://doi.org/10.5194/tc-2020-235
Preprint. Discussion started: 21 September 2020

basal friction under Ice Stream E (now known as MacAyeal Ice Stream). Since then, the use of inverse methods in estimating basal and internal conditions of glaciers from measured surface velocities has become widespread, supported by an increase in observational data from satellites and improvements in computational efficiency (Pattyn et al., 2017). The ability to perform large-scale inversions has revolutionised the field of ice flow modelling, allowing better representation of basal and rheological conditions to which the flow is sensitive. Several methods have been proposed and tested for models of varying complexity, including the adjoint method (MacAyeal, 1993) and subsequent variations (e.g., Vieli and Payne, 2003; Joughin et al., 2004; Petra et al., 2012; Morlighem et al., 2013; Perego et al., 2014), a least-squares inversion (Thorsteinsson et al., 2003), a non-linear Bayesian method (Raymond and Gudmundsson, 2009), inverse Robin problems (Arthern and Gudmundsson, 2010) and a nudging method (Mosbeux et al., 2016).

However, these inverse problems are not well posed and a unique solution is never guaranteed, regardless of the method used. In fact, a given inverse problem may have an infinite number of arbitrarily different solutions producing identical values in the forward problem (e.g., Zhdanov, 2015). An approach often used to remedy the ill-posedness of inverse problems is the introduction of regularisation, but there are many possible techniques for doing so. As such, the methods used and results obtained from inversions can differ considerably between models.

Aspects of inversion processes within individual models have been the subject of several recent studies. Koziol and Arnold (2017) incorporated subglacial hydrology into inversions for basal sliding. Kyrke-Smith et al. (2018) analysed the effects of basal topography on inversions. The sensitivity of inversions to several ice properties was tested by Zhao et al. (2018), and sensitivities at the surface to perturbations in basal conditions from inversions have been investigated by Martin and Monnier (2014) and Cheng and Lötstedt (2020). However, there are not many direct comparisons between inversions from different models. Morlighem et al. (2010) compared inversions using model equations of varying complexity, and the initMIP-Antarctica exercise Seroussi et al. (2019), as part of the ISMIP6 model intercomparison project, compared models which were set up using different datasets, with a focus on the responses in forward model runs to a variety of initialisation procedures.

The differences between outputs from different modelling platforms have not been given attention under controlled conditions, as it is generally thought that the products of inversions are highly model-dependent. In model intercomparison projects (e.g., Bindschadler et al., 2013; Asay-Davis et al., 2016) boundary conditions such as topography and melt rates are specified in detail, but participants are not given set values for the basal sliding coefficient or ice rheology rate factor. Instead, participants are asked to tune the initialisation of their models individually to set these values. This implies that the results of inversions are believed not to be purely representative of the physical properties of an ice flow, but also account for non-physical model behaviours resulting from different numerical implementations or approximations. We seek to test this belief, by comparing the outputs of carefully controlled inversions in different models.

https://doi.org/10.5194/tc-2020-235
Preprint. Discussion started: 21 September 2020

For this study, the focus is on inversions for basal sliding coefficients and ice rheology rate factor using an adjoint method, using the same input datasets. We compare the results of inversions from three ice flow models, identify the factors which cause differences between them and investigate the effect these differences have when transferring the products of inversions between models. We are interested in the extent to which the inversion processes are reflective of the physical ice flow described by the model equations, and by how much numerical model behaviour might be influencing the outputs. As part of this, we will assess whether the products of inversions can be used outside their model of origin, and whether the fields produced by inversions from different models result in the same behaviour in transient simulations. The more representative inversion processes are of the physical properties of the ice sheet system, the more similar their outputs should be.

Our chosen study area is the Amundsen Sea Embayment (ASE) in West Antarctica (Figure 1). Within this region, Thwaites Glacier is the subject of a targeted multidisciplinary investigation, the International Thwaites Glacier Collaboration (Scambos

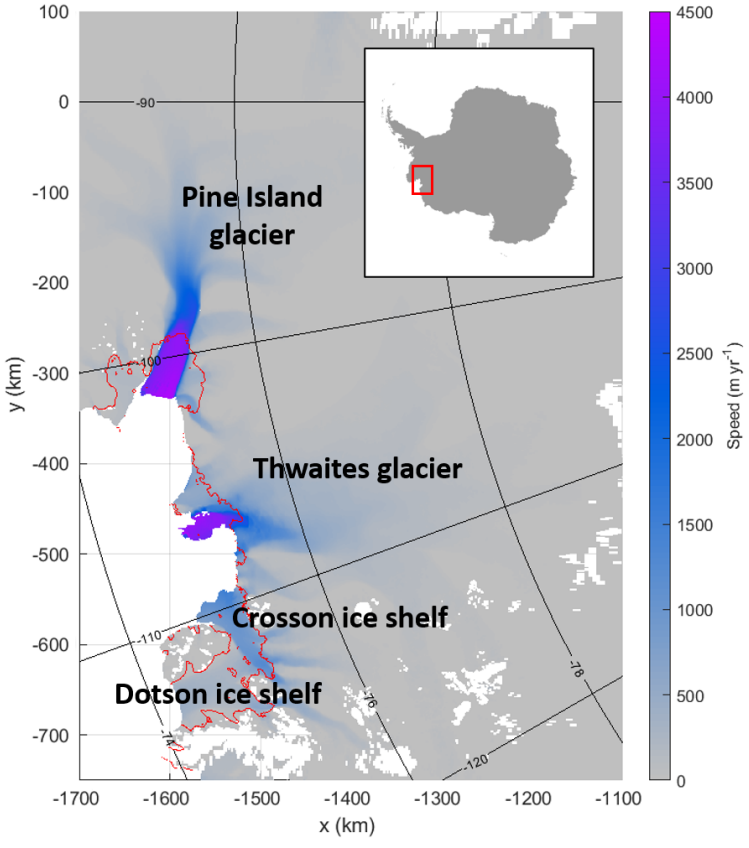

Figure 1. Amundsen Sea Embayment shaded with speed measurements from Mouginot et al. (2014). Grounding lines are shown in red.

https://doi.org/10.5194/tc-2020-235
Preprint. Discussion started: 21 September 2020

et al., 2017). Understanding change in the West Antarctic Ice Sheet has been identified as a top priority for future Antarctic research (National Academies of Sciences, Engineering, and Medicine, 2015). The Amundsen Sea, and Thwaites Glacier in particular, are of considerable interest due to rapid changes observed in the area over recent years (e.g., Mouginot et al., 2014; Milillo et al., 2019). Mass loss in the ASE is happening at a greater rate than anywhere else in Antarctica (Shepherd et al., 2018; Rignot et al., 2019), and has been accelerating (Sutterley et al., 2014). Many model simulations have been used to make predictions of the future evolution of Thwaites Glacier and the ASE region, and they can produce different results depending on model setup (e.g., Favier et al., 2014; Yu et al., 2018). However, these differences are predominantly in the rates of change rather than the direction of evolution. Forward simulations of ice flow models have been proved to be robust in intercomparison experiments, most recently MISMIP+ Cornford et al. (2020), and they generally agree that the trend of rapid retreat in the ASE will continue into the future (e.g., Joughin et al., 2014; DeConto and Pollard, 2016). There is a constant effort to improve the understanding and functionality of all aspects of ice flow models, and to reduce uncertainty in their predictions. Among the most important factors which models must account for, and which are challenging to obtain from direct observation, are ice rheology and basal conditions.

In this work, we start by giving details of the models used and their respective inversion procedures (section 2). We outline the experiments, along with the datasets and boundary conditions used, in section 3. Following this, output fields of speed misfit, rate factor and the basal sliding coefficient from inversions run in the three models are compared in section 4. In order to better understand how individual model behaviours affect inversion results, we then investigate specific factors which cause the differences. Finally, we run simulations using inversion outputs from all three models within the same time-evolving model, to assess the feasibility of transferring products of inversions between models and identify problems which may be encountered in doing so (section 5).

2 Model details

Three models are used in this study; Úa (Gudmundsson, 2020), the Ice-sheet and Sea-level System Model (Larour et al., 2012), known as ISSM, and the STREAMICE module of MITgcm (Goldberg and Heimbach, 2013). Úa and ISSM implement the Shallow Shelf Approximation (SSA) of MacAyeal (1989), and STREAMICE uses the L1L2 variant described in Goldberg (2011). Úa and ISSM employ unstructured meshes, which can be adapted to target specific areas of interest with finer resolution. STREAMICE, which inherits its grid and parallel domain decomposition from the MITgcm ocean model (Marshall et al., 1997), operates on a structured rectangular grid.

2.1 Parameters for inversion

Each model performs inversions for two parameters, a rheological parameter and a basal sliding coefficient. To describe ice rheology all models use the constitutive equation

$$\boldsymbol{\tau} = \frac{1}{2} A^{-\frac{1}{n}} \dot{\varepsilon}_e^{\frac{1-n}{n}} \dot{\boldsymbol{\varepsilon}} \tag{1}$$

https://doi.org/10.5194/tc-2020-235
Preprint. Discussion started: 21 September 2020


The Cryosphere Discussions

generally referred to in glaciology as the Glen's flow law (Glen, 1958), where $\dot{\boldsymbol{\varepsilon}}$ is the strain rate, $\dot{\varepsilon}_e$ is the effective strain rate, A is the ice flow rate factor, $\boldsymbol{\tau}$ is the deviatoric stress and n is a stress exponent. All the inversions in this study use the standard value of $n = 3$. Úa inverts for A or $\log_{10} A$, while ISSM inverts for a rheological parameter $B = A^{-\frac{1}{n}}$, sometimes known as the associated rate factor (eg., Greve and Blatter, 2009), and STREAMICE inverts for $\sqrt{B}$. The rate factors are an indicator of how soft or damaged ice is, with higher values of A corresponding to softer ice, and higher values of B corresponding to stiffer ice.

All three models employ the Weertman sliding law (Weertman, 1957), albeit in a slightly different form, as follows:

$$\text{Úa}: \quad \boldsymbol{\tau_b} = (C + C_0)^{-\frac{1}{m}} (\|\boldsymbol{v_b}\|^2 + v_0^2)^{\frac{1-m}{2m}} \boldsymbol{v_b} \tag{2}$$

$$\text{ISSM}: \quad \boldsymbol{\tau_b} = \beta^2 \|\boldsymbol{v_b}\|^{\frac{1}{m}-1} \boldsymbol{v_b} \tag{3}$$

$$\text{STREAMICE}: \quad \boldsymbol{\tau_b} = \beta^2 (\|\boldsymbol{v_b}\|^2 + v_0^2)^{\frac{1-m}{2m}} \boldsymbol{v_b}, \tag{4}$$

where $\boldsymbol{\tau_b}$ is the basal stress, $\boldsymbol{v_b}$ is the basal velocity, C_0 and v_0 are regularisation constants and m is the sliding law exponent, which in the case of these inversions is always $m = 3$. Úa inverts for either the basal sliding coefficient C, or $\log_{10} C$, while ISSM inverts for β^2, sometimes referred to as a basal friction or roughness coefficient, and STREAMICE inverts for β. In Úa, $C_0 = 1 \times 10^{-20}\ \text{kPa}^{-3}\,\text{m}\,\text{a}^{-1}$ and $v_0 = 1 \times 10^{-4}\ \text{m}\,\text{a}^{-1}$, and in STREAMICE, $v_0 = 1 \times 10^{-6}\ \text{m}\,\text{a}^{-1}$. ISSM does not employ a regularisation term in the sliding law, but the code contains a numerical verification which prevents division by zero.

2.2 Inversion methods

All of the inversion methods involve minimising a cost function of general form

$$\mathcal{J} = I + R,$$

where I is a misfit function and R is a regularisation term. The exact forms that these take varies. In the following, p refers to the parameters being inverted for, which differs between models. The observed values of surface velocities are u_{obs} and v_{obs}, in the x- and y-directions on a polar stereographic grid, with observational errors u_{err} and v_{err}.

2.2.1 Úa

In Úa, the cost function is $\mathcal{J}_{\text{Úa}} = I_{\text{Úa}} + R_{\text{Úa}}$. The misfit function is given by

$$I_{\text{Úa}} = \frac{1}{2\mathcal{A}} \int ((u - u_{\text{obs}})/u_{\text{err}})^2 \,\mathrm{d}s + \frac{1}{2\mathcal{A}} \int ((v - v_{\text{obs}})/v_{\text{err}})^2 \,\mathrm{d}s, \tag{5}$$

where $\mathcal{A}$ is the total area, u and v are the modelled horizontal velocity components and s is the ice surface.

https://doi.org/10.5194/tc-2020-235
Preprint. Discussion started: 21 September 2020

Úa employs Tikhonov regularisation, for which the regularisation term has the form

$$R_{\text{Úa}} = \sum_{k=1,2} \frac{1}{2\mathcal{A}} \int \left(\gamma_s^2 (\nabla (p_k - p_{k,\text{prior}}))^2 + \gamma_a^2 (p_k - p_{k,\text{prior}})^2 \right) \mathrm{d}s, \tag{6}$$

where γ_s and γ_a are the slope and amplitude regularisation parameters, $p_1 = \log_{10} A$, $p_2 = \log_{10} C$ and $p_{k,\text{prior}}$ are prior values, or initial estimates, for the parameters p_k. For the inversions in this report, $\gamma_s = 1 \times 10^4$ m and $\gamma_a = 1$, chosen after an L-curve analysis.

2.2.2 ISSM

In ISSM, the cost function is written as $\mathcal{J}_{\text{ISSM}} = I_{\text{ISSM}} + \alpha R_{\text{ISSM}}$, where α is the regularisation parameter. The misfit function is written as

$$I_{\text{ISSM}} = a I_{\text{abs}} + b I_{\log}, \tag{7}$$

where a and b are weighting parameters, with $b = 1$ being set and a adjusted such that the two components are equal in weight (within a given tolerance). I_{abs} and $I_{\log}$ are the absolute and logarithmic misfits given by

$$I_{\text{abs}} = \frac{1}{2} \int_s \left((u - u_{\text{obs}})^2 + (v - v_{\text{obs}})^2 \right) \mathrm{d}s \tag{8}$$

$$I_{\log} = \int_s \left(\log \left(\frac{\sqrt{u^2 + v^2} + \epsilon}{\sqrt{u_{\text{obs}}^2 + v_{\text{obs}}^2} + \epsilon} \right) \right)^2 \mathrm{d}s, \tag{9}$$

where ϵ is a minimum velocity applied to avoid numerical issues.

The regularisation term is defined as

$$R_{\text{ISSM}} = \frac{1}{2} \int_{\Omega_p} \|\nabla p\|^2 \, \mathrm{d}\Omega_p, \tag{10}$$

where Ω_p refers to the ice base when $p = \beta^2$, or to the ice volume when $p = B$.

In ISSM, the inversions for each parameter are carried out independently of each other. First, B is inverted for over a subdomain containing only the ice shelves, and then β^2 is inverted for on the grounded ice considering the whole domain, including the inverted value for B on the ice shelves. The regularisation term takes different values in each step, based on an L-curve analysis. For the B inversion $\alpha = 1 \times 10^{-18}$, and for the β^2 inversion $\alpha = 1 \times 10^{-8}$. Unless otherwise specified, B takes values calculated from the initial ISMIP6 temperatures (Seroussi et al., 2019) over the grounded ice, which are also used as priors for the floating ice.

https://doi.org/10.5194/tc-2020-235
Preprint. Discussion started: 21 September 2020


The Cryosphere Discussions

2.2.3 STREAMICE

In STREAMICE, the parameters inverted for are $p_1 = \sqrt{B}$ and $p_2 = \beta$. The cost function is $\mathcal{J}_{SI} = I_{SI} + R_{SI}$. Since STREAMICE is not a purely finite element model, the functions are written discretely, taking the form

$$I_{SI} = \sum_{i,j \in D} \frac{1}{2N} \left(\frac{(u(i,j) - u(i,j)_{\mathrm{obs}})^2 + (v(i,j) - v(i,j)_{\mathrm{obs}})^2}{(1 + (u^2_{\mathrm{err}_{i,j}} + v^2_{\mathrm{err}_{i,j}})^{\frac{1}{2}})^2} \right) \tag{11}$$

$$R_{SI} = \sum_{k=1,2} \sum_{i,j \in D} \frac{1}{N} \gamma_k \left(\left(\frac{p_k(i+1,j) - p_k(i,j)}{\Delta x(i,j)} \right)^2 + \left(\frac{p_k(i,j+1) - p_k(i,j)}{\Delta y(i,j)} \right)^2 \right) + \sum_{i,j \in D_G} \frac{1}{N} \gamma_G (p_1 - B_0)^2, \tag{12}$$

where i and j are grid cell indices, N is the total number of cells, Δx and Δy are the distances between grid cells in the x- and y-directions, $\mathcal{A}_{i,j}$ is the cell area, γ_1, γ_2 and γ_G are regularisation parameters, B_0 is an inital estimate for B, D is the full computational domain, and D_G consists of the grounded cells only. Note that the summations in I_{SI} and R_{SI} are not weighted by cell area, as they would be for a discretely calculated domain integral (*cf.* I_{ISSM} and $I_{\mathrm{Úa}}$). This is in order to prevent the inversion from weighting larger cells too strongly. For the inversions in this work, $\gamma_1 = \gamma_2 = 2 \times 10^4$ and $\gamma_G = 1 \times 10^2$. Unless otherwise specified, B_0 is calculated as a function of temperatures from Van Liefferinge and Pattyn (2013).

3 Experiment design and setup

3.1 Description of experiments

The first experiments involve a single inversion from each model. For the initial comparison, each model performs an inversion using the same geometry and velocity measurements, detailed in subsection 3.2. The resulting fields of rate factor and basal sliding coefficients are compared directly in order to see whether the models produce similar results. The velocity misfits, defined as the difference between the modelled and observed values, are also compared as an indicator of how well the inversion processes had performed. The results of this comparison are found in section 4.

Following this, further experiments seek to test the sensitivity of inversion outputs to particular details of the inversion procedure, such as the choices of optimisation scheme, algorithm sequence, mesh resolution and priors. An overview of the results of this study is found in subsection 4.4, and more detail is available in Appendix A.

The final stage (section 5) involves comparing the effects on the ice flow of using inversion outputs from each of the three models within a single model. The B and β^2 fields calculated by inversion in ISSM and STREAMICE are transferred into Úa and used as inputs for a set of simulations, alongside Úa's own inversion outputs. Firstly, time-independent diagnostic calculations are performed to identify any immediate differences in ice flow resulting from transferring the products of inversions

https://doi.org/10.5194/tc-2020-235
Preprint. Discussion started: 21 September 2020

between models. After this, the model is run forward in time to investigate the effects of using outputs from different models' inversions on the evolution of an ice flow model, with all else being equal.

3.2 Model domains and data

All three model domains used for our inversions, displayed in Figure 2, cover both Thwaites and Pine Island glaciers, and extend west to include the Dotson and Crosson ice shelves. They are set up using bedrock and ice surface fields linearly interpolated from BedMachine Antarctica (Morlighem et al., 2019). The inversions use the surface velocities and measurement error from the 2014-15 year of the updated dataset originally described in Mouginot et al. (2014). The same velocities and geometries are used throughout this study in all models. The densities are set to be constant and uniform, with values of $917\,\mathrm{kg\,m^{-3}}$ for ice density and $1027\,\mathrm{kg\,m^{-3}}$ for ocean water density, which are the values used in the hydrostatic equilibrium calculation for BedMachine.

The STREAMICE domain is a 528×720 cell rectangular grid, with a minimum resolution of $1\,\mathrm{km}$ at the centre of the domain, and maximum resolution at the edges of $5.4\,\mathrm{km}$ in the x-direction and $5.96\,\mathrm{km}$ in the y-direction. The other two models use triangular meshes with spatially varying resolution. Both have a finer resolution closer to the grounding line. The ISSM mesh contains 261,375 elements with edge lengths between $725\,\mathrm{m}$ on the ice shelf and $16\,\mathrm{km}$ in the coarsest areas, with a resolution of about $1\,\mathrm{km}$ close to the grounding line. The mesh was refined based on the distance from the grounding line and

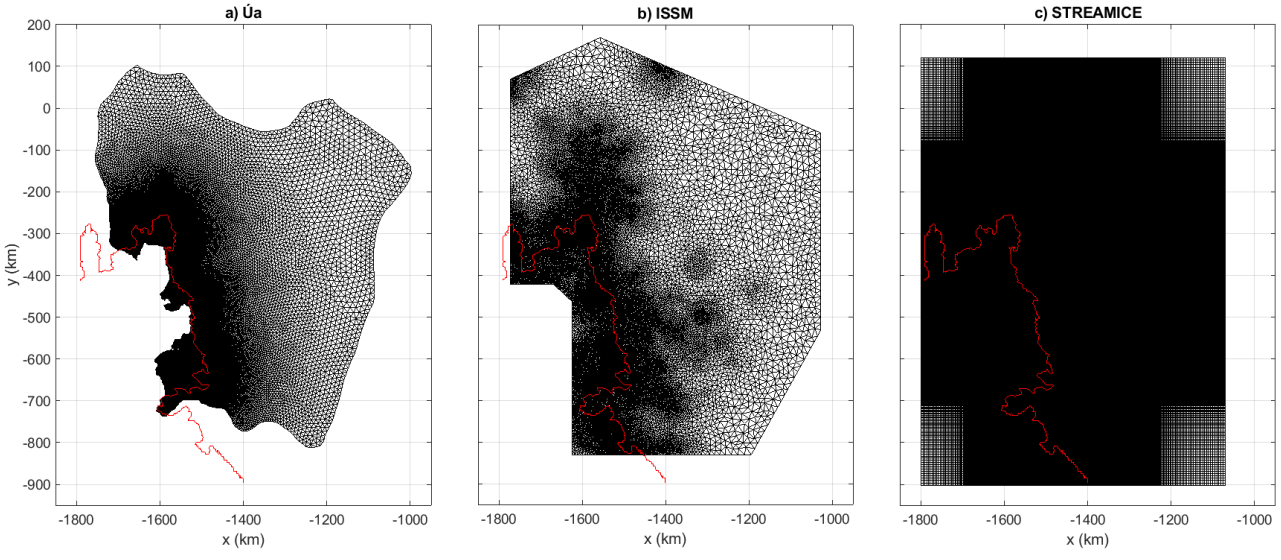

Figure 2. The meshes used by each model for the inversions. All domains cover our area of interest including Pine Island and Thwaites glaciers, and the Dotson and Crosson ice shelves. The main grounding line is shown in red.

https://doi.org/10.5194/tc-2020-235
Preprint. Discussion started: 21 September 2020


The Cryosphere Discussions

interpolation error of the observed ice velocity. The Úa mesh contains 213,828 elements with edge lengths varying linearly with the distance from the grounding line and additional refinement of areas with high velocity or strain rates, with resolution varying from 500 m to 15 km. The Úa mesh boundary was chosen based on the drainage basins of the glaciers and the location of the ice front, while the other two meshes cover larger areas which contain this region of interest. The triangular meshes used were created using BAMG (Hecht, 2006) in ISSM and Mesh2D (Engwirda, 2014) in Úa.

For some experiments, we used coarser versions of the Úa mesh, which we refer to as 'Mesh2' and 'Mesh3'. These have the same boundary, but are designed to have element edge lengths two and three times those of the original Úa mesh. Thus, Mesh2 contains 58,292 elements with edge lengths between 1 km and 30 km, and Mesh3 contains 30.421 elements with edge lengths between 1.5 km and 45 km.

The forward simulations were run using 'Mesh2'. Surface mass balance for these experiments is from a climatological record of RACMO2.1 (Lenaerts et al., 2012). For basal melting of the ice shelf we use the simple depth-based parameterisation

$$m_b = \begin{cases} 0 & \text{if } z \geq 0 \\ -\frac{75}{500} z & \text{if } 0 > z > -500 \\ 75 & \text{if } z \leq -500, \end{cases} \tag{13}$$

where m_b is the basal melt rate in $\mathrm{m\,a^{-1}}$ and z is the vertical coordinate in metres, positive upwards with zero at sea level.

4 Results of inversions

We first look at the outputs from inversions run in the three ice flow models following the procedures previously described. The fields we compare are the speed misfit, and the values of B and β^2. The outputs from all three models were converted to common units of $\mathrm{Pa\,a^{\frac{1}{3}}}$ for B and $\mathrm{Pa\,m^{-\frac{1}{3}}\,a^{\frac{1}{3}}}$ for β^2. These are the units used for all comparisons in this work.

For the purpose of the comparisons in this section, outputs from Úa and ISSM were interpolated linearly onto the rectangular grid of the STREAMICE domain. As can be seen from the shapes of the domains in Figure 2, this results in some areas containing extrapolated values. Any area where this is the case has been masked out in figures, such that they display only the region for which directly calculated values are available. The ice mask for the STREAMICE domain has also been applied.

https://doi.org/10.5194/tc-2020-235
Preprint. Discussion started: 21 September 2020

The Cryosphere Discussions
Open Access
EGU

4.1 Speed misfit

Speeds $V = \sqrt{u^2 + v^2}$ and $V_{\mathrm{obs}} = \sqrt{u_{\mathrm{obs}}^2 + v_{\mathrm{obs}}^2}$ were calculated. The difference between modelled and observed speed, which we refer to as the misfit, is $V_{\mathrm{diff}} = V - V_{\mathrm{obs}}$.

The speed misfits for each model are displayed in Figure 3. The speed misfit is a useful quantity to inspect in order to ensure that the inverted values of B and β^2 produce reasonable velocities, but the exact magnitudes are not necessarily indicative of the quality of the inversions themselves. As shown in subsection 2.2, the cost functions being minimised balance misfit and regularisation, thus different choices of regularisation in each inversion affect the misfit produced. The most important thing to note is that none of the inversions produce velocities which do not resemble the observations.

A visual comparison reveals that Úa has minimised the difference furthest, with misfit under $50\,\mathrm{m\,a^{-1}}$, except in localised spots such as the edge of the Thwaites Ice Tongue. The misfit of STREAMICE does not exceed $200\,\mathrm{m\,a^{-1}}$ in general, again with a few small exceptions. ISSM displays higher misfits of hundreds of metres per year, particularly on the Thwaites Ice Tongue. The mean magnitudes of velocity misfit across the entire domain are $7.10\,\mathrm{m\,a^{-1}}$ for Úa, $15.61\,\mathrm{m\,a^{-1}}$ for STREAMICE and $19.43\,\mathrm{m\,a^{-1}}$ for ISSM, highlighting the differences we can visibly see between the models. In general across all three models, the greatest differences are seen on the floating ice downstream of the grounding line, and on the fastest flowing grounded ice.

While we can see similarities in the locations of high misfit regions, the overall correlation between the distributions of misfit is not high. We calculated the Pearson correlation coefficient (Pearson, 1895) between each pair of misfit fields, and

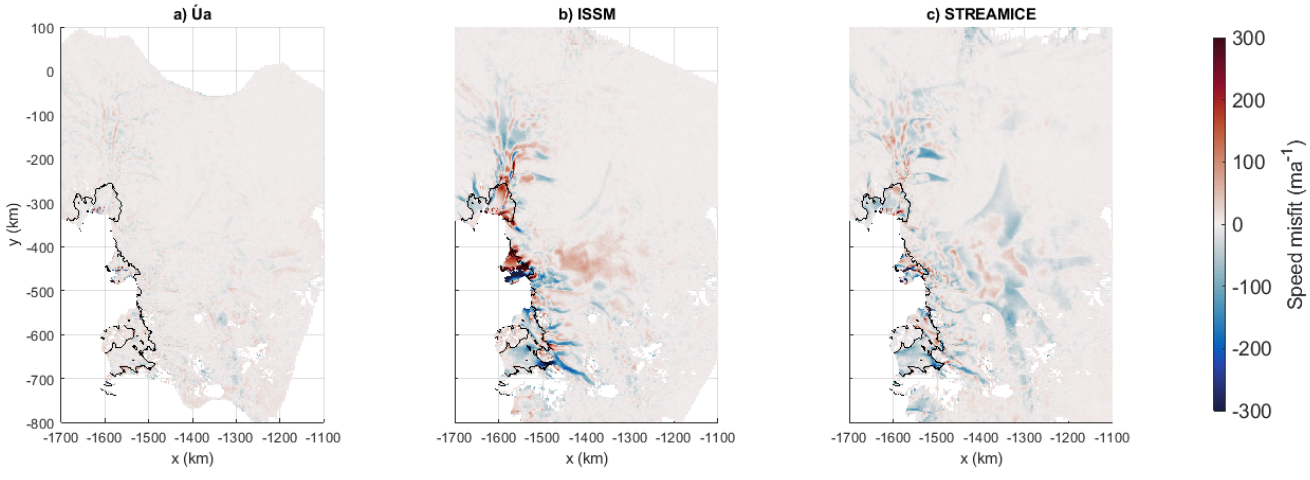

Figure 3. Difference in the calculated speeds after inversion, compared to the measurements, for each model. The grounding line is indicated in black.

https://doi.org/10.5194/tc-2020-235
Preprint. Discussion started: 21 September 2020

found the most similar to be Úa and STREAMICE, with a coefficient of 0.474. ISSM has a lower positive correlation with each of the other models, with coefficients of 0.276 and 0.270 for STREAMICE and Úa respectively. We note that these correlation coefficients serve only as rough quantitative estimates of the correlations between different inversion products. In general, we expect the correlation to depend on the spatial scales considered. For example, and as indicated by our inversion results, we generally observe better agreement over large spatial scales ($\geq 50\,\mathrm{km}$)) than over smaller spatial scales.

4.2 Associated rate factor, B

The results from the rate factor inversion (Figure 4) show the most widespread differences between the models. All the models produce values of similar magnitude, but the values in Úa are spread over a larger range and the field is less smooth. The smoother fields produced by ISSM and STREAMICE can be explained by the fact that these models do not generally invert for B over grounded ice, as described in section 2. Instead, both models calculate their priors from temperature, with STREAMICE using temperatures from Van Liefferinge and Pattyn (2013) and ISSM following the process described in Seroussi et al. (2019). STREAMICE does allow for some perturbation from the initial values on grounded ice if significant changes are needed to minimise the velocity misfit, but this is heavily restricted by the last term in Eq. (12). Meanwhile Úa, which allows optimisation of the rate factor over the entire domain, produces a much more spatially variable field over the grounded ice. This is likely due in part to differences in regularisation applied in this particular example rather than a general feature. Locally, values of B from Úa's inversion are up to an order of magnitude different from the prescribed temperature-based estimates used by the other two models.

On floating ice, ISSM and STREAMICE produce similar results, with differences between their outputs (Figure 4(d-f)) generally being small. The Úa output differs from the other two, producing a more variable distribution over the ice shelves, as it does over the grounded sections. Úa's inversion produces softer ice on the Western ice shelf of Thwaites and close to the calving front of Crosson ice shelf. However, it does also produce some similar features, with bands of softer ice being visible at the edges of the high-velocity ice streams which flow out onto Pine Island and Thwaites ice shelves. In general, the bigger differences are seen in faster-flowing areas, with the values for B being most similar over Dotson ice shelf and the northern section of the Pine Island ice shelf, both of which have low measured surface velocities.

To provide some quantification of the differences between the rate factor fields calculated by the models, we use Pearson correlation coefficients as before. The coefficient values can be found in Table 1. Over the entire domain, the distribution produced by Úa is almost entirely uncorrelated with the output from the other two models. ISSM and STREAMICE, by contrast, are fairly well correlated, despite using different temperature fields to calculate the value on the grounded ice. When looking only at the floating ice, Úa shows a moderate positive correlation with the other models. This demonstrates a fairly significant effect of Úa performing the inversion for rate factor over the entire domain compared to the approaches of the other models.

https://doi.org/10.5194/tc-2020-235
Preprint. Discussion started: 21 September 2020

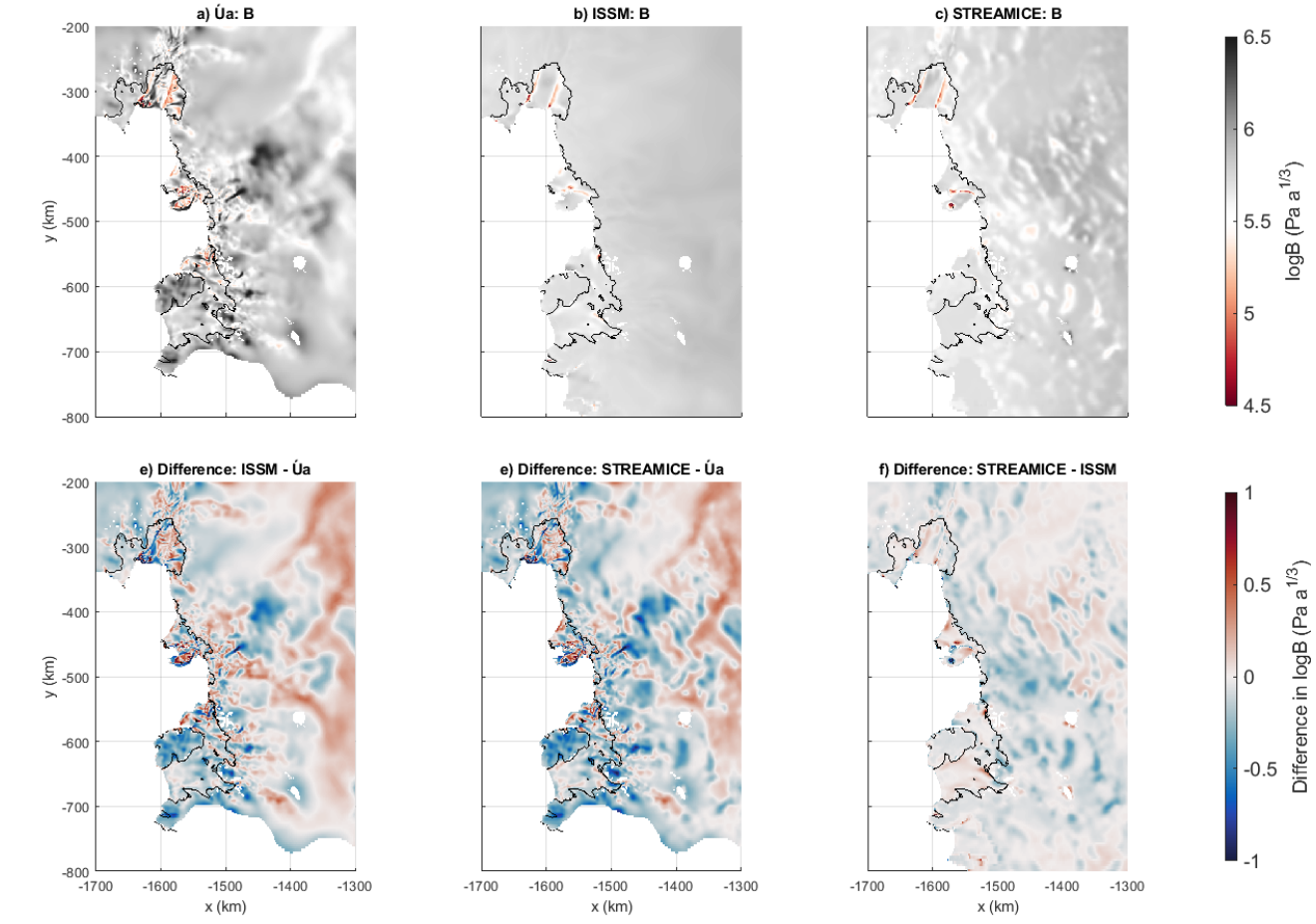

Figure 4. The B fields calculated by inversion and differences between them, displayed on a logarithmic colour scale in units of $\mathrm{Pa\,a^{\frac{1}{3}}}$. The grounding line is indicated in black.

4.3 Basal friction coefficient, β^2

Inverted β^2 fields (Figure 5) show a greater agreement between models than the B inversion products. This is likely because all three models are inverting for the parameter over the entire domain. An implication of this is that the inverted β^2 values appear not to be significantly dependent on the values of B, or on whether or not the two inversions were performed simultaneously.

However, there are still some notable differences between the β^2 fields. When compared to Úa, ISSM and STREAMICE have patches of lower β^2 values over the trunk of Pine Island glacier which are less than $1\ \mathrm{m^{-\frac{1}{3}}\,a^{\frac{1}{3}}}$. Also, in all three difference plots (Figure 5(d-f)), there are localised larger differences in the immediate vicinity the grounding line. The STREAMICE output occasionally contains loops of lower values. These appear due to the model inverting for β rather than β^2, and in some

https://doi.org/10.5194/tc-2020-235
Preprint. Discussion started: 21 September 2020

locations producing values of β below zero, which is not physically viable. Thus when β^2 is calculated from the output, ensuring positive values everywhere, the shape of the function is changed to include peaks inside the rings of low values, rather than the local minima represented in the original inversion for β.

Once again, calculating Pearson correlation coefficients between the outputs gives us a quantitative idea of how alike the distributions are. We find strong positive correlation coefficients in the region of 0.8 for each comparison pair (see Table 1 for exact values). This shows a high level of agreement between the β^2 outputs of different inversion processes, suggesting that the underlying physics of the model equations are well represented in these results.

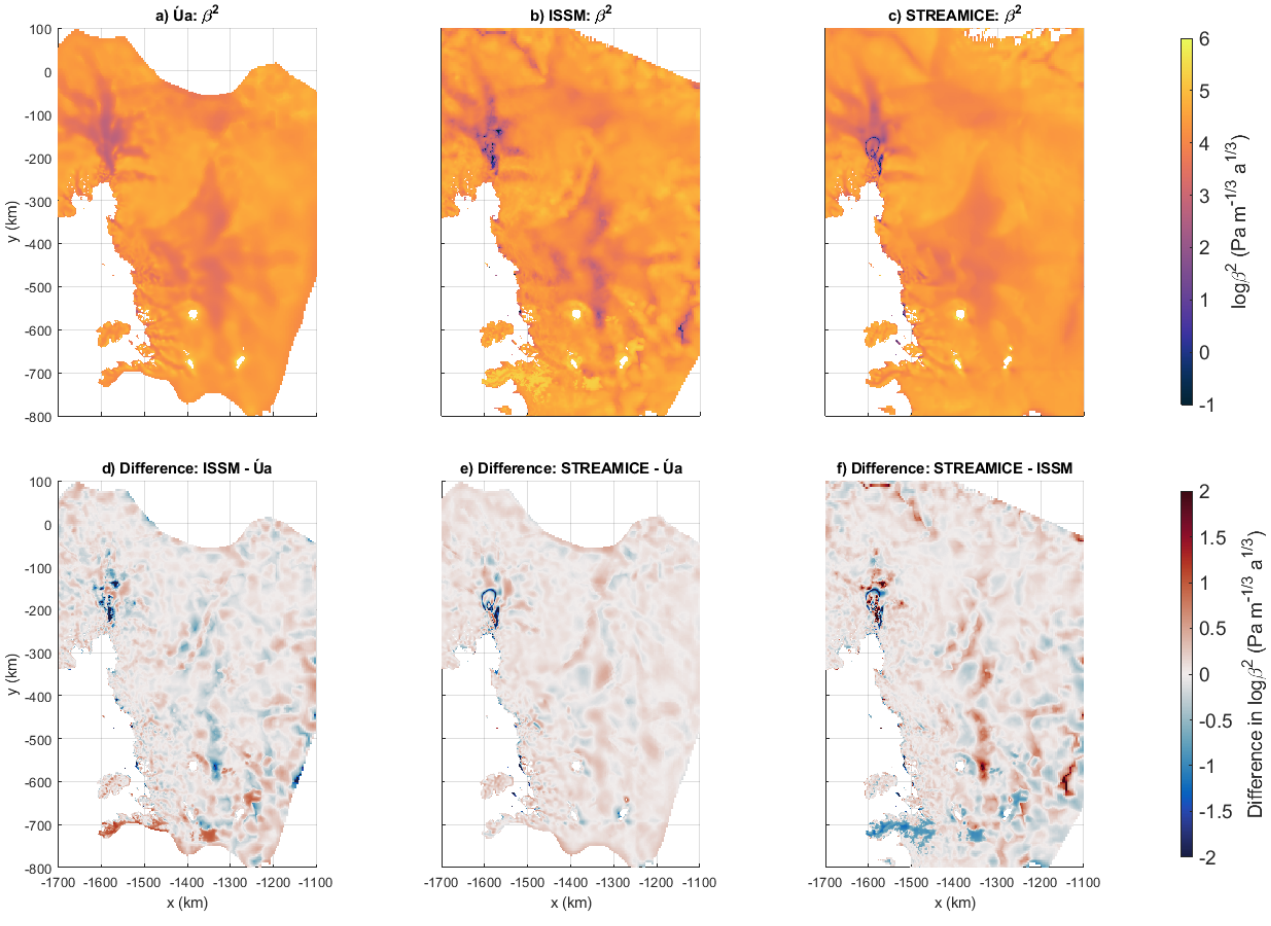

Figure 5. The β^2 fields calculated by inversion and differences between them, displayed on a logarithmic colour scale in units of $\mathrm{Pa\,m^{-\frac{1}{3}}\,a^{\frac{1}{3}}}$. The ungrounded area of the domain has been masked out.

https://doi.org/10.5194/tc-2020-235
Preprint. Discussion started: 21 September 2020


The Cryosphere Discussions
Open Access
EGU

	Úa & ISSM	Úa & STREAMICE	ISSM & STREAMICE
Speed misfit correlation	0.270	0.474	0.276
B correlation (whole domain)	0.077	0.058	0.666
B correlation (floating ice only)	0.368	0.340	0.511
β^2	0.843	0.871	0.798

Table 1. Pearson correlation coefficients calculated for different inversion outputs between all model pairs.

4.4 Discussion of inversion outputs

There are many factors which could cause differences in inversions. We have investigated several of these within Úa in an attempt to identify in particular why the difference in the misfit produced by Úa's inversions is lower than the other two models, and what causes patches of lower β^2 values to be produced over Pine Island. We summarise the findings here, but further details of this investigation can be found in Appendix A.

The difference in misfit appears to be due to a combination of factors. As noted in subsection 4.1, it may just be a symptom of different regularisation choices between the models. However, we have identified other factors which may contribute to the difference. ISSM and STREAMICE use a different optimisation scheme, which results in a higher misfit when tested in Úa. However, the B and β^2 fields from these experiments correlate well with Úa's original result, so the optimisation scheme does not account for the differences found in these outputs. Differences in meshes and the choice of priors were also tested and not found to cause significant changes to the inversion results, except in cases where the parameters were beyond the range of variation in our original inversions.

Major factors affecting the inversion results appear to be the section of the domain over which B is inverted for, and the non-sequential nature of ISSM's inversion. Úa produces higher misfit when inverting only for β^2 with a predetermined B field. In the β^2 field, patches of lower values are produced in a similar location over Pine Island to those noted in subsection 4.3. The outputs from the experiment in which this was tested had lower correlations with the original inversion than those of any other experiments.

In general, the inversions were found to agree on large-scale distributions of B on the ice shelves, and of β^2 everywhere. Due to our careful control of input datasets, we have removed much of the variability which can be introduced between models in general usage, and have shown the outputs to be robust with respect to technical aspects of the inversion process. An implication we take from this is that our inversion outputs are representative of the physics of the underlying equations rather than individual numerical details in the model code. Given the similarities in the inversion outputs, it may be possible to transfer them between models and recover broadly similar results in forward simulation. This is what we attempt next.

https://doi.org/10.5194/tc-2020-235
Preprint. Discussion started: 21 September 2020


The Cryosphere Discussions

5 Transferring inversion outputs between models

5.1 Diagnostic calculations

A diagnostic model step calculates an instantaneous velocity from the given boundary conditions and geometry, without any time evolution. It is the same calculation performed during iterations of the inversion process. Our calculations are performed on 'Mesh2', a coarser version of the Úa mesh with minimum edge lengths of 1 km. In doing so, the Úa inversion outputs are interpolated onto a mesh which was not originally used to calculate them, in the same way as those from the other models, which should reduce any effects of discrepancies in re-meshing and interpolation on our comparisons. This choice also serves the purpose of ensuring that the resolution of the mesh is similar to that of the coarsest of the three inversion outputs. The boundary of the mesh is based on the edges of drainage basins as before, and we use a Dirichlet boundary condition to set velocities along it to zero.

To test the compatibility of our inversion outputs between models, we ran diagnostic calculations in Úa using the fields of B and β^2 produced by all three models as properties of the ice. In doing so, we observed how large the impact of differences in underlying model processes can be. These calculations produce velocity fields which vary significantly between simulations, despite all inputs other than the rate factor and basal sliding coefficient being identical. Differences are seen in particular on the fastest flowing ice, and on the ice shelves.

We find that the different methods of grounding line regularisation employed by the models are a major cause of discrepancies on the ice shelves. Changing a regularisation parameter in Úa allows us to better match the velocities produced by the other models' inversions in an attempt to replicate their own regularisation as closely as possible within Úa's framework. By choosing the value of this parameter, we are able to ensure that the velocities calculated using each set of inversions match closely over the ice shelves, where the effect of the regularisation is most prominent. Details of the grounding line regularisation methods, and their effects on both diagnostic calculations and time-dependent simulations, can be found in Appendix B.

The differences encountered indicate that transferring inversion products between models may not necessarily be a simple matter. Changing the grounding line regularisation parameter can greatly improve the diagnostic values over ice shelves, but this is an ad-hoc approach not based on the physical equations of the system. Differences on the grounded ice are unaccounted for by this process, as seen in Figure 6. All sets of inversion outputs, including those from Úa when interpolated to Mesh2, produce higher velocities over the grounded region compared to the original velocity measurements. This is at least partly due to the interpolation of fields onto a new mesh, as evidenced by Úa's inversion outputs displaying the behaviour, albeit to a lesser extent. The fact that STREAMICE appears to be the worst affected may be due to its mesh being the most different.

https://doi.org/10.5194/tc-2020-235
Preprint. Discussion started: 21 September 2020

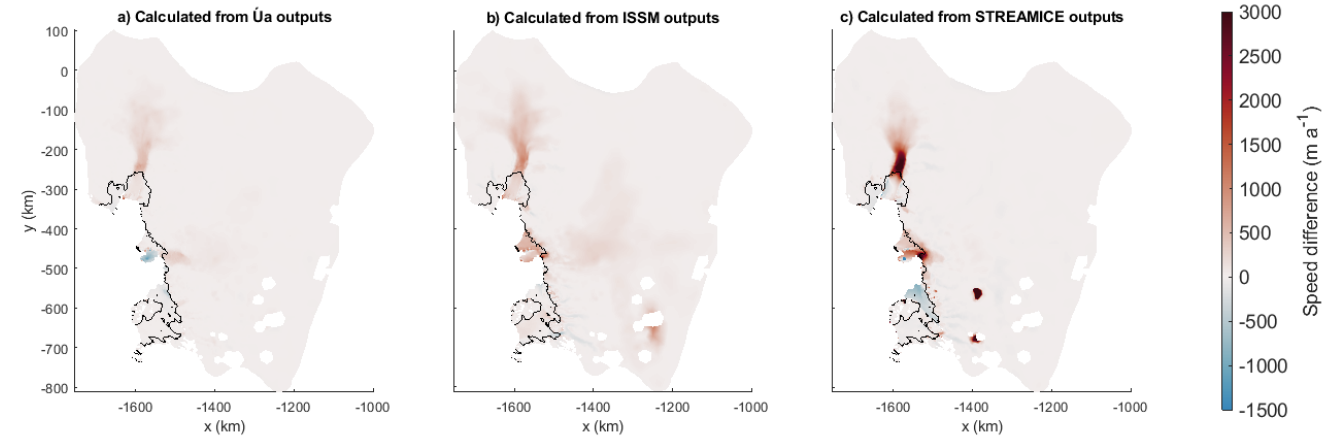

Figure 6. Differences between the speed calculated diagnostically in Úa using the B and β^2 outputs from each model, and the original speed measurements used for the inversions.

A conclusion we can come to from the experiments discussed in Appendix B is that the comparison of diagnostic velocities is not in fact a good indicator of performance in a time-dependent run. The large velocity differences in these diagnostic calculations do not necessarily mean that similarly large differences will be present in forward simulations.

5.2 Time-dependent runs

We performed three time-dependent simulations in Úa, using each pair of inversion products as inputs for the rate factor and basal sliding coefficient. In each case, the model was allowed to evolve for 40 years from the initial state described by our geometry datasets. Like the diagnostic calculations, these simulations were run on Mesh2. Following the results of Appendix B, the grounding line regularisation parameter was not altered between experiments, and thus the only differences between these simulations are the B and β^2 fields.

The evolution of the ice sheet follows a similar trajectory with each pair of fields for rate factor and basal sliding coefficients. However, the changes happen at different rates. The ice loss over the domain is displayed in Figure 7(a-b), where we see that the rate of mass loss is faster using the fields calculated by STREAMICE and ISSM. We also see differences in the grounded area (Figure 7(c)). All three simulations again display the same behaviour, with the grounded area increasing during the first 5-10 years before starting to decrease, with the system evolving at different rates. More ice becomes ungrounded when using the STREAMICE inversion outputs, as is particularly evident in the position of the grounding line of Thwaites Glacier in Figure 8. This figure also displays the thickness changes over the 40 years of simulation. We see more thinning of the ice sheets in the simulation using the STREAMICE inversion outputs, but similar patterns in all three cases.

https://doi.org/10.5194/tc-2020-235
Preprint. Discussion started: 21 September 2020

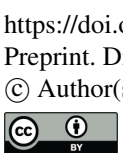

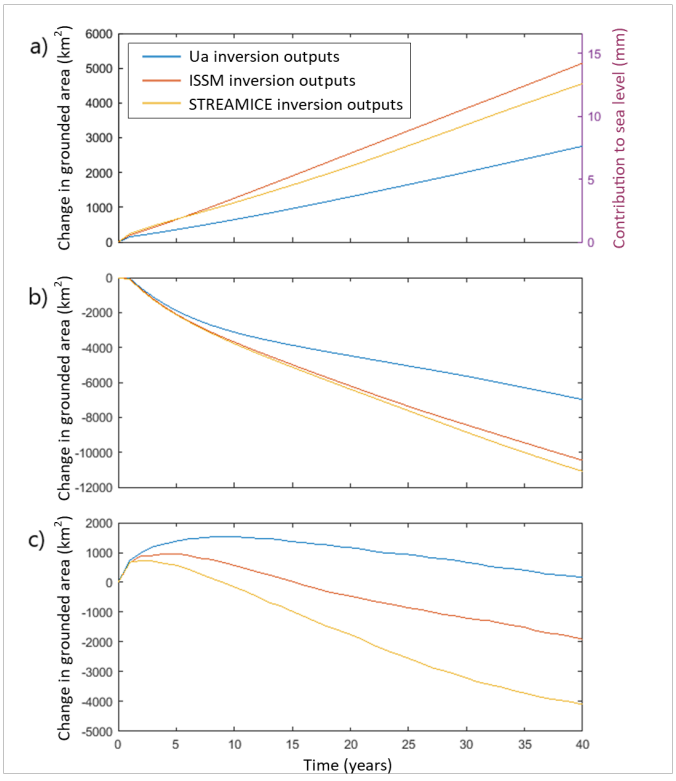

Figure 7. Changes in mass loss and grounded area over 40 years of simulation in Úa using the rate factor and basal sliding coefficient fields resulting from each of the three model inversions.

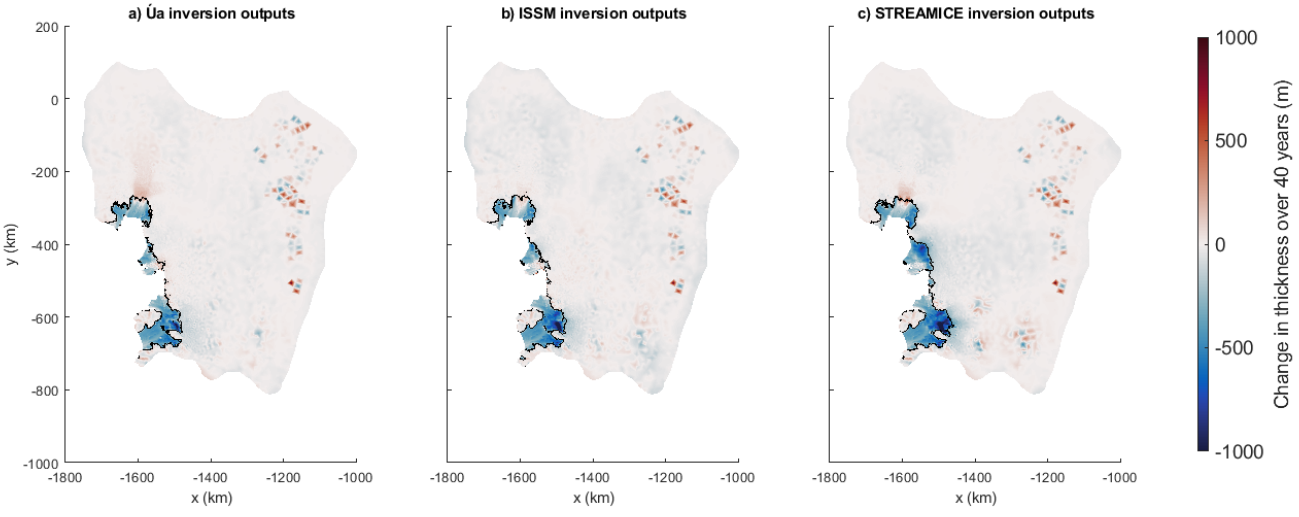

Figure 8. Thickness and grounding line changes after 40 years of simulation in Úa using the rate factor and basal sliding coefficient fields resulting from each of the three model inversions.

https://doi.org/10.5194/tc-2020-235
Preprint. Discussion started: 21 September 2020

After 40 years, the contributions to sea level calculated using the three sets of model inversions differ by up to 7 mm, a factor of two. Although quite a large difference, this range compares favourably to differences between model initialisations studied in the control experiment of initMIP-Antarctica (Seroussi et al., 2019). The variability in ice mass loss is also less than that of Alevropoulos-Borrill et al. (2020), in which sensitivity of simulations to basal sliding and rate factor were tested by perturbing the fields, and less than the variability between models in the experiments of Favier et al. (2014), Bindschadler et al. (2013) or (Levermann et al., 2020). These favourable comparisons demonstrate the value of the standardisation of input datasets in our inversions, which helps to minimise uncertainty when transferring them. The difference between values for contribution to sea level also fall within the ranges reported in other studies assessing different aspects of models, suggesting that the uncertainties introduced by using these inversion products outside of their native model are not more than those of, for example, the different climate forcings used in LARMIP-2 (Levermann et al., 2020) or the choice of sliding law in Yu et al. (2018).

6 Conclusions

In this work, we have investigated the differences between inversions for flow rate factor and basal sliding coefficients calculated in three different ice flow models. They each use different methods and employ different techniques during the inversion process. Upon inspection the outputs from these inversions display a high degree of agreement in patterns of distribution, with strong positive correlations particularly evident between the fields of basal sliding coefficients, for which some differences at smaller scales can be attributed to various technical aspects of the models. The rate factor inversions showed slightly less agreement, suggesting that B is less closely linked to surface velocities than β^2.

The implication of these findings is that results of inversions do contain some representation of numerical behaviour, but much more strongly reflect the underlying physics of the equation system the models are designed to solve. The results of inversion processes used by these models are shown to be consistent with each other to a higher extent than may have been expected from the ill-posedness of the problem being solved. The minimal model-dependence demonstrates that ice flow models are as robust in their inversions as they are in their forward simulations.

Further to this, we have shown that the products of inversions from one model can be transferred into another model. It may not always be a simple matter, however, and care must be taken when doing so. In our case, diagnostic calculations were particularly affected by different representations of the grounding line within the models, and by interpolation onto a different mesh. Other models may present different challenges to overcome. In order to successfully transfer the product of an inversion out of its native model, technical knowledge of both the original and host models will be required.

Due to our careful control of input datasets, the results of our time-dependent simulations show variability lower than those of other intercomparison experiments. In theory, with provision of sufficient technical details of the models involved, it should

https://doi.org/10.5194/tc-2020-235
Preprint. Discussion started: 21 September 2020

be possible to produce fields of basal sliding coefficients and rate factors which could be used by multiple models for the purpose of increasing uniformity in the boundary conditions and ice properties of intercomparison projects.

Code availability. Source code for Úa can be downloaded at http://doi.org/10.5281/zenodo.3706623, and requires MATLAB to run. Source code for ISSM can be downloaded at https://issm.jpl.nasa.gov/download. STREAMICE is part of MITgcm, for which the source code is found at http://mitgcm.org/source-code.

Appendix A: Investigating the effects of differing aspects of model inversion processes

After observing the differences between the inversion results of the three ice flow models, we investigated possible causes for them. Each of the models approaches the inversion process in a slightly different way, and further testing would reveal which factors are the most influential in affecting the outcome. We tested different factors by performing independent inversion calculations for each case in Úa, and in one case across all three models. We looked at the velocity misfits, rate factors and basal sliding coefficients produced as indicators of inversion performance compared to the original results. We attempted to determine from this how robust our inversion results are with respect to these procedural differences.

A1 Optimisation schemes

One possible source of inconsistency between the models is the optimisation scheme used during the inversion process. ISSM and STREAMICE both make use of a scheme called M1QN3 (Gilbert and Lemaréchal, 1989), while Úa uses the Interior Point algorithm (Byrd et al., 1999) via MATLAB's inbuilt 'fmincon' function. Since Úa appeared to be performing better in minimising the differences between modelled and observed velocities, this was an important operational difference to check. We compared these algorithms in Úa by using a MATLAB implementation of M1QN3 from the OPTI Toolbox (Currie and Wilson, 2012). Used on the same inversion problem, M1QN3 under-performed compared to Interior Point algorithm. The inversion process aborted after 601 iterations, with the cost function having converged to a minimum value of 13.96, while the Interior Point algorithm reduced the cost function to 11.64 in the same number of iterations. The Interior Point algorithm continued to further minimise the cost function until the process was stopped at the 1000 iteration limit set in Úa, at which point the cost function value was 10.12. The minimisation processes for both algorithms are shown in Figure A1.

The misfit fields resulting from these inversions (Figure A2(b)) do not show a great enough difference in magnitude to entirely account for the discrepancies observed between the inversions from different models. While the M1QN3 inversion is visibly performing less well than MATLAB's Interior Point scheme, the misfit is smaller than those seen in results from the two models using M1QN3 by default. The mean magnitude of misfit using M1QN3 is $9.61\,\mathrm{m\,a^{-1}}$, so by this measure it could account for roughly 30% of the difference observed between Úa and STREAMICE in subsection 4.1, and 20% of the difference seen in ISSM. In this case, as opposed to in the original inversion comparisons, the misfit is a more direct indicator

https://doi.org/10.5194/tc-2020-235
Preprint. Discussion started: 21 September 2020

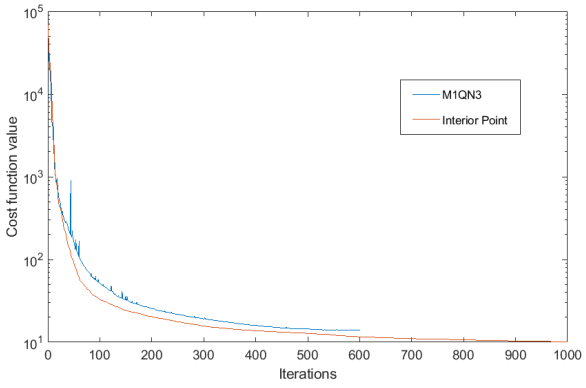

Figure A1. A comparison of the performance of the Interior Point algorithm in MATLAB used by default in Úa, and the M1QN3 optimisation scheme used by ISSM and STREAMICE, showing minimisation of the cost function during the inversion process.

of performance. Since the regularisation is exactly the same in both cases, the only differences in misfit are due to the choice of optimisation scheme.

It is interesting to note that use of the M1QN3 algorithm results in slightly lower values of β^2 on part of Pine Island glacier, in a similar location to the low-value patches seen on the ISSM and STREAMICE inversions. The earlier termination of the minimisation process compared to Úa's Interior Point algorithm could be a cause of differences in that area. On the whole, however, there is a strong positive correlation in the spatial distribution of both the basal sliding coefficients and the speed misfit when comparing the two optimisation algorithms, with a weaker correlation in the rate factor. The correlation coefficients for several experiments described in this appendix can be found in Table A1.

A2 Inverting for basal sliding alone

The way in which ISSM performs its B and β^2 inversions sequentially rather than simultaneously and, in common with STREAMICE, does not generally invert for B over the grounded ice, could impact the result. To test this, we took the result of the B inversion from ISSM and used it as an input for an inversion in Úa. In this experiment, Úa was used to invert only for basal sliding coefficient, without changing the rate factor.

The results of this test (Figure A2(c)) show that using ISSM's calculated B field causes larger misfits in the velocity of the floating ice, especially on the Thwaites Ice Tongue. This is consistent with differences seen in the original misfit comparison (subsection 4.1). Some of those differences also propagate upstream of the grounding line. Fixing B to the values calculated from a temperature field causes a patch of low β^2 values to form over Pine Island glacier, in a similar way to the original results from the ISSM and STREAMICE inversions. The values dip below $10^2\ \mathrm{m}^{-\frac{1}{3}}\ \mathrm{a}^{\frac{1}{3}}$, but do not reach the lowest values found in the original results. It appears that Úa's usual method of inverting for both parameters across the entire domain causes

https://doi.org/10.5194/tc-2020-235
Preprint. Discussion started: 21 September 2020

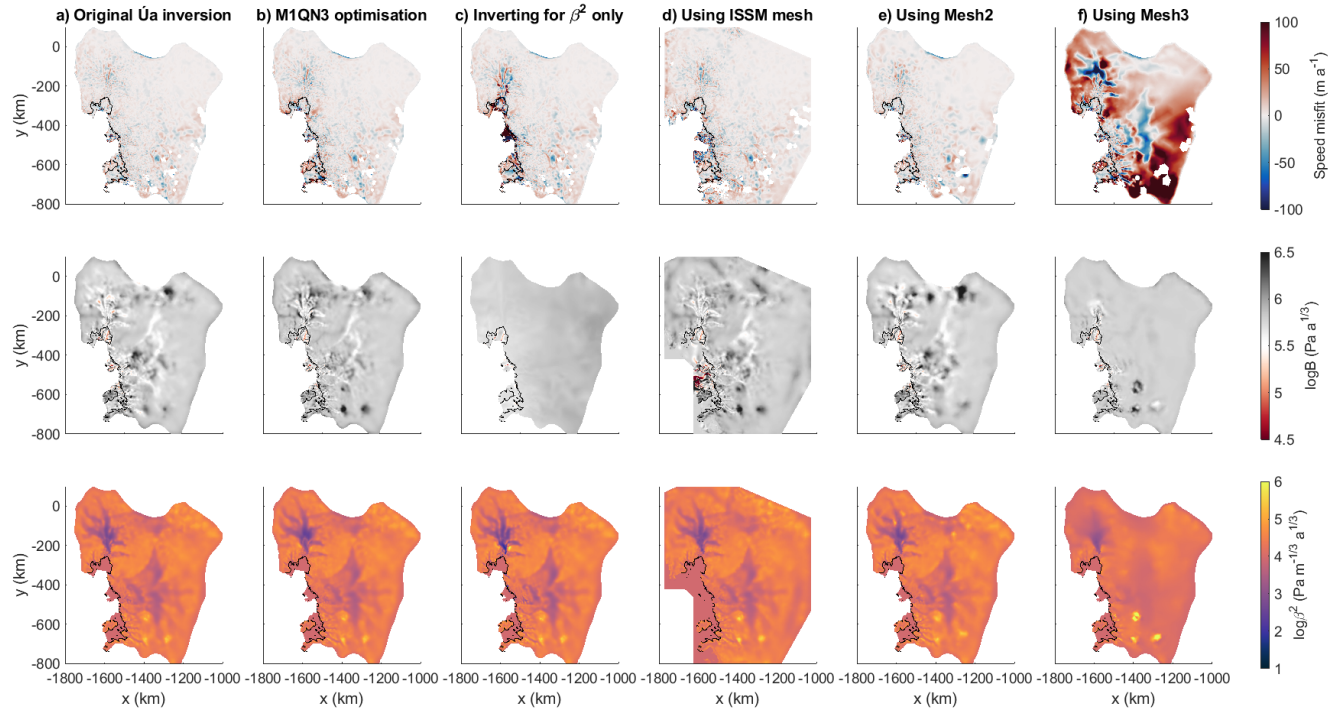

Figure A2. A comparison of the speed misfit, rate factor and basal sliding coefficients for several cases of inversions run in Úa under different conditions. Column a) The original Úa inversion for B and β^2 using an Interior Point optimisation scheme. Column b) The inversion using M1QN3 optimisation scheme. Column c) Inverting for β^2 only, using ISSM's B field. Column d) Using the mesh and domain of the original ISSM inversion. Column e) Using the second (coarser) version of Úa's mesh. Column f) Using the third (even coarser) version of Úa's mesh.

information which would otherwise be interpreted as extreme lows in the β^2 field be be absorbed into the B values instead. This can explain some of the differences seen in the original inversions.

The calculated correlation of β^2 with the outputs of the original Úa inversion is very low, despite a visual inspection of the results showing similarities and familiar features. This is caused by localised spikes of extreme values affecting the calculation. Once the β^2 field is edited to remove these extreme values, by capping values at 1×10^6 Pa m$^{-\frac{1}{3}}$ a$^{\frac{1}{3}}$, the correlation coefficient is recalculated as 0.512. This is in the region which would be expected from visual inspection of Figure A2, although still a weaker correlation than those found for other factors under investigation. The issue of localised extreme values affecting the correlation is one which is also encountered for the B field, and in further results of this appendix. They are indicated in Table A1.

https://doi.org/10.5194/tc-2020-235
Preprint. Discussion started: 21 September 2020

The Cryosphere Discussions

	ISSM	STREAMICE	M1QN3	β^2 only	ISSM mesh	Mesh2	Mesh3
Speed misfit correlation	0.270	0.474	0.980	0.021	0.743	0.963	0.863
B correlation (whole domain)	0.077	0.058	0.449	0.076*	0.389*	0.220*	0.238*
B correlation (floating ice only)	0.368	0.340	0.455	0.116*	0.350*	0.206*	0.236*
β^2 correlation	0.843	0.871	0.914	0.512†	0.929	0.945	0.552†

Table A1. The Pearson correlation coefficients of various models and tests with Úa's original inversion. The first two columns show the correlation of the original ISSM and STREAMICE inversions, and the remaining columns show the correlation with the cases displayed in Figure A2(b-f). *Values limited to 5×10^7 $\mathrm{Pa\,a^{\frac{1}{3}}}$ before calculating correlation. †Values limited to 1×10^6 $\mathrm{Pa\,m^{-\frac{1}{3}}\,a^{\frac{1}{3}}}$ before calculating correlation.

A3 Mesh and resolution

The models are performing their calculations over different meshes, so experiments to test the mesh-dependence of inversions were performed. We first tested the mesh of ISSM within Úa, and found that the inversion outputs are not particularly sensitive to the location of mesh points if the resolutions are similar as is the case here. A comparison produced a strong positive correlation in the β^2 and misfit distributions, with Figure A2(d) showing that there is not a large difference in the velocity misfit. The results for B show greater variation.

The minimum length of the elements in Úa's original mesh is 500 m, but STREAMICE uses a mesh with minimum resolution of 1 km. STREAMICE uses rectangular elements in its mesh which Úa cannot replicate, so instead we looked at the effects of changing the mesh resolution. Performing the same inversion in Úa over different resolutions shows some interesting results. 'Mesh2' is created with element edge lengths twice that of the original Úa mesh, and 'Mesh3' with three times the original lengths. An inversion over Mesh2 produces a slightly larger misfit (Figure A2(e)) than the original mesh, but the distribution of the misfit field correlates strongly with that calculated on the original mesh. There is also a high correlation between the β^2 fields produced in each case, with the differences between the two cases being primarily apparent in the B field.

Using Mesh3 (Figure A2(f)), which has minimum element edge lengths of 1.5 km, we see a much greater difference. In this case the misfit is far higher, and there are noticeable differences in the fields of B and β^2, which are lacking much of the detail present when using the other meshes. This shows that there is a limit to the mesh resolution from which useful inversion results can be obtained using the same settings.

Within the range of resolutions of our models in their original states, the inversions for β^2 are robust and consistent. However, the results of the experiment using Mesh3 show that inversions performed on meshes with significantly lower mesh resolutions do not retain this consistency. The inversions for B appear to be more mesh-dependent, with far lower correlation.

https://doi.org/10.5194/tc-2020-235
Preprint. Discussion started: 21 September 2020

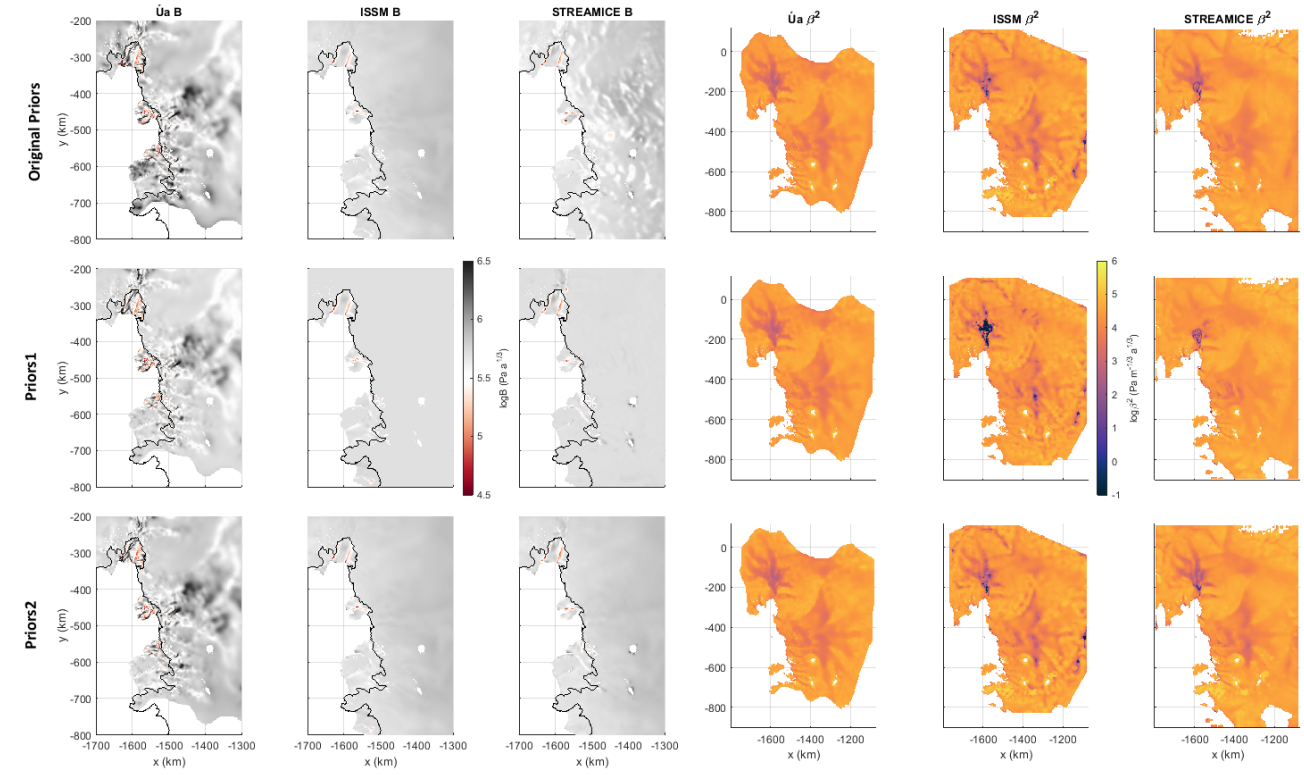

Figure A3. A comparison of the outputs of inversions using the original priors from each model in the first row, and the two specified sets, Priors1 and Priors2, in the second and third rows.

A4 Priors

In the original inversion comparison, each model was given the freedom to pick its own default priors for B and β^2. This choice of a starting point for the inversion could have an effect on the outcome. To test this, two inversions were run in each model with identical priors. One set of priors (Priors1) consists of uniform values for B and β^2, such that $\log(B) = 5.7$ and $\log(\beta^2) = 4.3$. The other (Priors2) consists of ISSM's original prior for B, and a β^2 field calculated using the Weertman sliding law with our velocity dataset and a constant value of $\tau_b = 80\,\mathrm{kPa}$.

The results in Figure A3 show that all models have some dependency on the priors chosen. In general, the rate factor is most heavily influenced by the prior field used, due to two of the models not changing these initial values over much of the domain. Even in Úa, which does invert for B everywhere, the influence of the prior values can clearly be seen on the slow-flowing ice inland. Pearson correlation coefficients for B are found in Table A2. Looking at the floating ice only, using the same priors across all three models does not have a significant effect on the correlation of B distribution between Úa and either of the other

https://doi.org/10.5194/tc-2020-235
Preprint. Discussion started: 21 September 2020

The Cryosphere Discussions
Open Access
EGU

	Úa			ISSM			STREAMICE		
	Original	Priors1	Priors2	Original	Priors1	Priors2	Original	Priors1	Priors2
Úa Original		0.794	0.793	0.077	0.204	0.077	0.058	0.274	0.127
Úa Priors1	0.817		0.772	0.099	0.175	0.099	0.056	0.219	0.134
Úa Priors2	0.794	0.864		0.424	0.226	0.424	0.317	0.299	0.455
ISSM Original	0.368	0.365	0.353		0.526	1.000	0.666	0.424	0.932
ISSM Priors1	0.374	0.358	0.329	0.901		0.526	0.238	0.626	0.434
ISSM Priors2	0.368	0.365	0.353	1.000	0.901		0.666	0.424	0.932
STREAMICE Original	0.340	0.334	0.313	0.511	0.550	0.511		0.399	0.726
STREAMICE Priors1	0.433	0.423	0.387	0.657	0.729	0.657	0.794		0.583
STREAMICE Priors2	0.455	0.353	0.423	0.712	0.697	0.712	0.744	0.941	

Table A2. The Pearson correlation coefficients for B between pairs of tests using different sets of priors. Above the diagonal are coefficients calculated over the entire domain. Below the diagonal are the coefficients calculated over the floating ice only.

	Úa			ISSM			STREAMICE		
	Original	Priors1	Priors2	Original	Priors1	Priors2	Original	Priors1	Priors2
Úa Original		0.989	0.970	0.843	0.715	0.819	0.871	0.732	0.885
Úa Priors1	0.953		0.984	0.838	0.722	0.813	0.864	0.729	0.883
Úa Priors2	0.952	0.956		0.835	0.698	0.808	0.850	0.726	0.886
ISSM Original	0.270	0.264	0.265		0.749	0.971	0.798	0.669	0.867
ISSM Priors1	0.217	0.219	0.210	0.747		0.748	0.681	0.520	0.688
ISSM Priors2	0.280	0.272	0.273	0.958	0.755		0.779	0.664	0.847
STREAMICE Original	0.474	0.463	0.463	0.276	0.220	0.274		0.815	0.904
STREAMICE Priors1	0.324	0.321	0.305	0.186	0.118	0.148	0.407		0.781
STREAMICE Priors2	0.633	0.630	0.639	0.329	0.249	0.324	0.687	0.428	

Table A3. The Pearson correlation coefficients for β^2 and speed misfit between pairs of tests using different sets of priors. Above the diagonal are coefficients calculated for β^2. Below the diagonal are the coefficients calculated for speed misfit.

https://doi.org/10.5194/tc-2020-235
Preprint. Discussion started: 21 September 2020

models. However, there is a noticeable strengthening of the correlation between the inverted values of ISSM and STREAMICE over the ice shelves using both Priors1 and Priors2.

In the β^2 results, we find a slightly different outcome. Úa's results are affected very little by changing the priors, whereas the original outputs from ISSM and STREAMICE show a greater correlation with the outputs using Priors2. The difference can be seen in Figure A3 most prominently over Pine Island glacier. These results tell us that Úa is the least sensitive model to a change in priors, but also that the choice of priors is only a matter for concern in STREAMICE and ISSM if a reasonable field cannot be calculated from existing velocity or temperature data. Even the lowest correlation in Table A3, between ISSM and STREAMICE both using Priors1, is greater than 0.5.

The strong correlations between each model's original output and the Priors2 experiments leads us to conclude that the choice of priors is not a major factor in the differences between the original inversions, as neither STREAMICE nor ISSM was using uniform priors.

Appendix B: The effects of grounding line parameterisation when transferring inversion outputs

B1 Differences in diagnostic calculations

Diagnostic calculations performed in Úa using the fields of B and β^2 from each of the three models revealed large discrepancies between the velocity fields produced. The velocities produced when using the inversion outputs from ISSM and STREAMICE were significantly greater in magnitude than those calculated by their native models.

After some experimentation, it was found that an influencing factor behind the differences on the ice shelves was the value of Úa's grounding line regularisation parameter, `kH`. By changing this paramenter, the magnitude of diagnostically calculated velocities could be altered to better reproduce those of the other models using their own inversion outputs. The reason for this is that our three models use different regularisation methods in the definition of the grounding line. Inversions in STREAMICE are calculated using a flotation relationship containing a Heaviside function which indicates whether ice in a mesh element is floating or grounded. Úa uses a modified version of this, smoothing the Heaviside function by use of the `kH` parameter to avoid discontinuities which would cause problems in the model's numerical processes. ISSM uses the sub-element parameterisation scheme SEP2, as described in Seroussi et al. (2014). The purpose of models regularising in this way is one of numerical convenience rather than physical accuracy.

The exact position of the grounding line is a very important factor in ice flow modelling. In our case, the differences between grounding line regularisation across the models are probably the cause of the slightly higher differences in the β^2 fields close to the grounding line noted in subsection 4.3. These differences in β^2 then translate to differences in the velocities calculated

https://doi.org/10.5194/tc-2020-235
Preprint. Discussion started: 21 September 2020

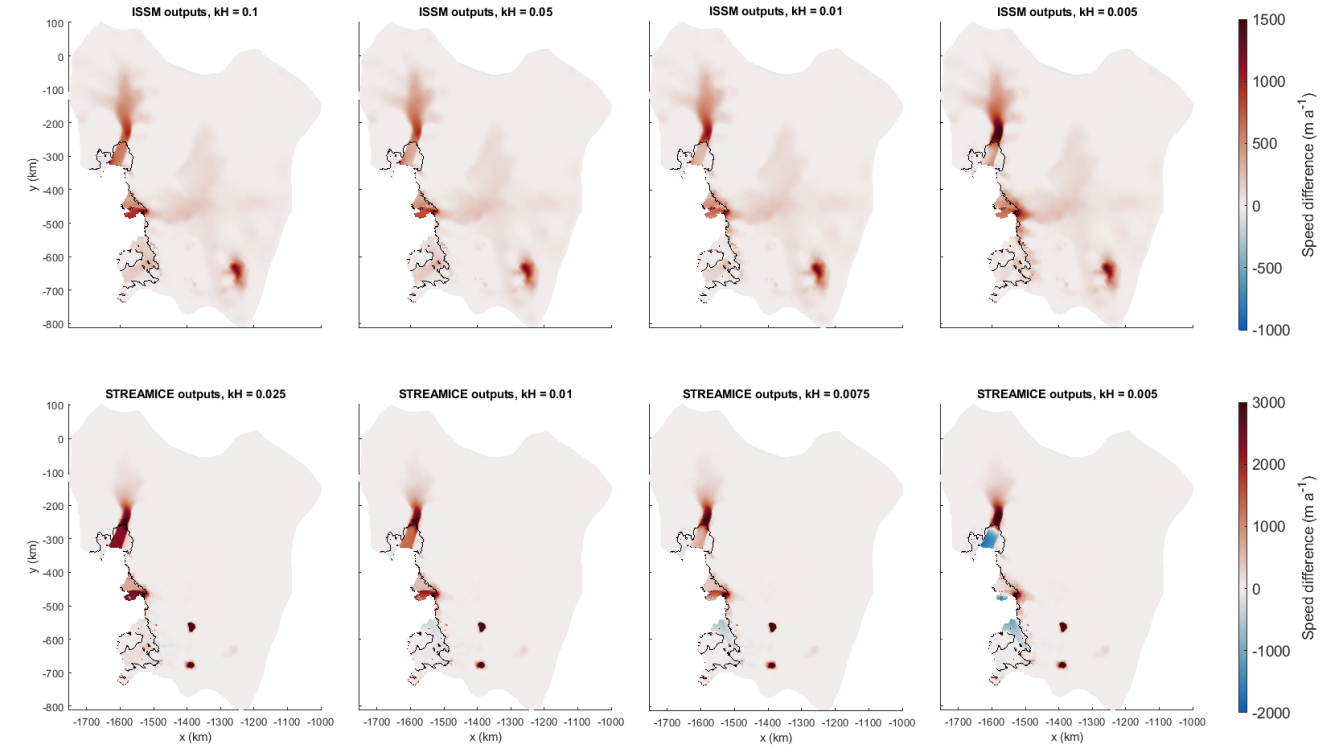

Figure B1. Differences between diagnostic speeds calculated in Úa using the ISSM and STREAMICE inversion outputs and a range of values for `kH`, and the speeds calculated in the original models. Note that each row uses a different colour scale.

from the ISSM and STREAMICE fields in Úa, where the grounding line is defined slightly differently.

Figure B1 displays the differences between diagnostic speeds calculated in Úa and those calculated in the models from which the inversion outputs originate. A range of `kH` values are used, showing the effect of changing this parameter. Lower values of `kH` indicate that the Heaviside function in the flotation relationship is smoothed over a greater distance.

For the ISSM outputs, lowering the value of `kH` causes the difference in calculated velocity to decrease on the ice shelf. However, there is a 'tipping point' beyond which decreasing the value further starts to increase the difference in the calculated velocity everywhere, especially on the grounded ice. For the results displayed in Figure 6 (subsection 5.1), we chose to set `kH` such that the difference on the ice shelf was minimised but this 'tipping point' was not passed, at $\texttt{kH} = 0.02$.

The STREAMICE outputs follow a slightly different pattern. Beyond the 'tipping point', the difference on the ice shelves continues to follow the same trajectory, becoming negative as `kH` is lowered further. The change in the differences around this 'tipping point' is more sudden, and the difference on the grounded ice is greater in magnitude that that of the ISSM outputs.

https://doi.org/10.5194/tc-2020-235
Preprint. Discussion started: 21 September 2020

Note that for these reasons, the bottom row of Figure B1 uses a different colour scale and different values of kH than the top row. The value chosen for the results displayed in Figure 6 was $\mathrm{kH} = 0.0065$.

B2 Effects on time-dependent simulations

The effect of the grounding line regularisation is different in time-dependent simulations. This is best illustrated by the comparisons of speed and grounding line position shown in Figure B2. This displays the results of three different simulations run in Úa, at one year and ten years. The first is using Úa's own fields for B and β^2, while the other two use the fields calculated by inversion in ISSM. The latter two are run using different values for kH: one with $\mathrm{kH} = 0.02$, the value chosen for the diagnostic calculation, and one with $\mathrm{kH} = 1$, the value used in the Úa simulation.

With both values for kH, the ISSM fields produce a higher velocity. However, the difference is larger when using the value which we chose for diagnostic calculations. We see that in the case where $\mathrm{kH} = 0.02$, the grounding line moves much further

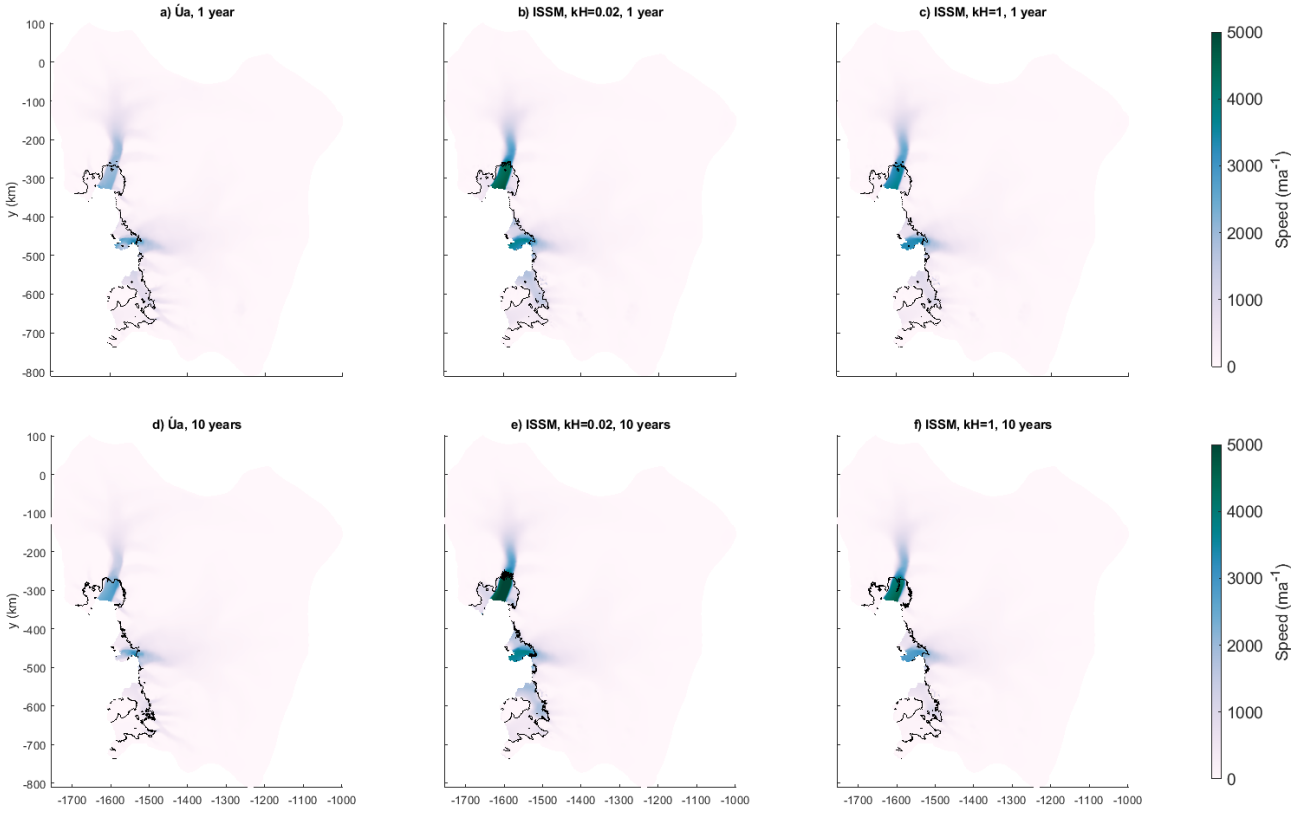

Figure B2. Speeds and grounding lines after 1 and 10 years of simulation in Úa using its own inversion outputs, and those of ISSM with two different values of kH.

https://doi.org/10.5194/tc-2020-235
Preprint. Discussion started: 21 September 2020

from its position in the simulation run using Úa's inversion outputs. This suggests that in forward runs, the value of `kH` should be kept consistent over simulations, and that the effects of changing it in the diagnostic calculations are not indicative of performance in time-dependent simulations.

The effects of using different values of `kH` are not unexpected, as it is a regularisation parameter rather than a physical property of the ice. The definition of the grounding line has a large effect on where basal melting is applied, which is not included in the diagnostic calculation, and any grounding line regularisation will introduce errors. Thus for the time-dependent comparisons in subsection 5.2, the value of `kH` should be the same in all cases, and sufficiently large, to ensure consistency and accuracy in the physics involved in mass balance. The error introduced by different grounding line parameterisations being used in the creation of B and β^2 fields is smaller than the error introduced by using different grounding line regularisation parameters in time-dependent simulations. As a consequence, the results of our diagnostic calculations are not indicative of performance in forward runs.

Author contributions. All authors were involved in the conception of the project, and discussions throughout. JMB coordinated the project, and carried out the modelling work in Úa. TDdS and DG carried out the modelling work in ISSM and STREAMICE respectively. JMB led the writing of the manuscript, and all authors provided comments and feedback during the editing process.

Competing interests. The authors declare that they have no competing interests.

Acknowledgements. This work is from the PROPHET project, a component of the International Thwaites Glacier Collaboration (ITGC). Support from National Science Foundation (NSF: Grant #1739031) and Natural Environment Research Council (NERC: Grants NE/S006745/1, NE/S006796/1 and NE/T001607/1). ITGC Contribution No. 019.

https://doi.org/10.5194/tc-2020-235
Preprint. Discussion started: 21 September 2020

References

Alevropoulos-Borrill, A. V., Nias, I. J., Payne, A. J., Golledge, N. R., and Bingham, R. J.: Ocean-forced evolution of the Amundsen Sea catchment, West Antarctica, by 2100., The Cryosphere, 14, 2020.

Arthern, R. J. and Gudmundsson, G. H.: Initialization of ice-sheet forecasts viewed as an inverse Robin problem, Journal of Glaciology, 56, 527–533, 2010.

Asay-Davis, X. S., Cornford, S. L., Durand, G., Galton-Fenzi, B. K., Gladstone, R. M., Gudmundsson, G. H., Hattermann, T., Holland, D. M., Holland, D., Holland, P. R., et al.: Experimental design for three interrelated marine ice sheet and ocean model intercomparison projects: MISMIP v. 3 (MISMIP+), ISOMIP v. 2 (ISOMIP+) and MISOMIP v. 1 (MISOMIP1), Geoscientific Model Development, 9, 2471–2497, 2016.

Bindschadler, R. A., Nowicki, S., Abe-Ouchi, A., Aschwanden, A., Choi, H., Fastook, J., Granzow, G., Greve, R., Gutowski, G., Herzfeld, U., et al.: Ice-sheet model sensitivities to environmental forcing and their use in projecting future sea level (the SeaRISE project), Journal of Glaciology, 59, 195–224, 2013.

Byrd, R. H., Hribar, M. E., and Nocedal, J.: An interior point algorithm for large-scale nonlinear programming, SIAM Journal on Optimization, 9, 877–900, 1999.

Cheng, G. and Lötstedt, P.: Parameter sensitivity analysis of dynamic ice sheet models–numerical computations, The Cryosphere, 14, 673–691, 2020.

Cornford, S. L., Seroussi, H., Asay-Davis, X. S., Gudmundsson, G. H., Arthern, R., Borstad, C., Christmann, J., Dias dos Santos, T., Feldmann, J., Goldberg, D., Hoffman, M. J., Humbert, A., Kleiner, T., Leguy, G., Lipscomb, W. H., Merino, N., Durand, G., Morlighem, M., Pollard, D., Rückamp, M., Williams, C. R., and Yu, H.: Results of the third Marine Ice Sheet Model Intercomparison Project (MISMIP+), The Cryosphere, 14, 2283–2301, https://doi.org/10.5194/tc-14-2283-2020, https://tc.copernicus.org/articles/14/2283/2020/, 2020.

Currie, J. and Wilson, D. I.: OPTI: Lowering the Barrier Between Open Source Optimizers and the Industrial MATLAB User, in: Foundations of Computer-Aided Process Operations, edited by Sahinidis, N. and Pinto, J., Savannah, Georgia, USA, 2012.

DeConto, R. M. and Pollard, D.: Contribution of Antarctica to past and future sea-level rise, Nature, 531, 591–597, 2016.

Engwirda, D.: Locally optimal Delaunay-refinement and optimisation-based mesh generation, Ph.D. thesis, School of Mathematics and Statistics, The University of Sydney, 2014.

Favier, L., Durand, G., Cornford, S. L., Gudmundsson, G. H., Gagliardini, O., Gillet-Chaulet, F., Zwinger, T., Payne, A., and Le Brocq, A. M.: Retreat of Pine Island Glacier controlled by marine ice-sheet instability, Nature Climate Change, 4, 117–121, 2014.

Gilbert, J. C. and Lemaréchal, C.: Some numerical experiments with variable-storage quasi-Newton algorithms, Mathematical programming, 45, 407–435, 1989.

Glen, J.: The flow law of ice: A discussion of the assumptions made in glacier theory, their experimental foundations and consequences, IASH Publ, 47, e183, 1958.

Goldberg, D. and Heimbach, P.: Parameter and state estimation with a time-dependent adjoint marine ice sheet model, The Cryosphere, 7, 1659–1678, 2013.

Goldberg, D. N.: A variationally derived, depth-integrated approximation to a higher-order glaciological flow model, Journal of Glaciology, 57, 157–170, 2011.

Greve, R. and Blatter, H.: Dynamics of ice sheets and glaciers, Springer Science & Business Media, 2009.

Gudmundsson, G. H.: GHilmarG/UaSource: Ua2019b (Version v2019b), http://doi.org/10.5281/zenodo.3706623, 2020.

https://doi.org/10.5194/tc-2020-235
Preprint. Discussion started: 21 September 2020

Hecht, F.: BAMG: Bidimensional Anisotropic Mesh Generator, Tech. rep., FreeFem++, 2006.

Joughin, I., MacAyeal, D. R., and Tulaczyk, S.: Basal shear stress of the Ross ice streams from control method inversions, Journal of Geophysical Research: Solid Earth, 109, 2004.

Joughin, I., Smith, B. E., and Medley, B.: Marine ice sheet collapse potentially under way for the Thwaites Glacier Basin, West Antarctica, Science, 344, 735–738, 2014.

Koziol, C. P. and Arnold, N.: Incorporating modelled subglacial hydrology into inversions for basal drag, The Cryosphere, 11, 2783–2783, 2017.

Kyrke-Smith, T. M., Gudmundsson, G. H., and Farrell, P. E.: Relevance of detail in basal topography for basal slipperiness inversions: a case study on Pine Island Glacier, Antarctica, Frontiers in Earth Science, 6, 33, 2018.

Larour, E., Seroussi, H., Morlighem, M., and Rignot, E.: Continental scale, high order, high spatial resolution, ice sheet modeling using the Ice Sheet System Model (ISSM), Journal of Geophysical Research: Earth Surface, 117, 2012.

Lenaerts, J. T., Van den Broeke, M., Van de Berg, W., Van Meijgaard, E., and Kuipers Munneke, P.: A new, high-resolution surface mass balance map of Antarctica (1979–2010) based on regional atmospheric climate modeling, Geophysical Research Letters, 39, 2012.

Levermann, A., Winkelmann, R., Albrecht, T., Goelzer, H., Golledge, N. R., Greve, R., Huybrechts, P., Jordan, J., Leguy, G., Martin, D., et al.: Projecting Antarctica's contribution to future sea level rise from basal ice shelf melt using linear response functions of 16 ice sheet models (LARMIP-2), Earth System Dynamics, 11, 35–76, 2020.

MacAyeal, D. R.: Large-scale ice flow over a viscous basal sediment: Theory and application to ice stream B, Antarctica, Journal of Geophysical Research: Solid Earth, 94, 4071–4087, 1989.

MacAyeal, D. R.: The basal stress distribution of ice stream E, Antarctica, inferred by control methods, Journal of Geophysical Research, https://doi.org/10.1029/91JB02454, 1992.

MacAyeal, D. R.: A tutorial on the use of control methods in ice-sheet modeling, Journal of Glaciology, 39, 91–98, 1993.

Marshall, J., Hill, C., Perelman, L., and Adcroft, A.: Hydrostatic, quasi-hydrostatic, and nonhydrostatic ocean modeling, Journal of Geophysical Research: Oceans, 102, 5733–5752, https://doi.org/10.1029/96JC02776, http://dx.doi.org/10.1029/96JC02776, 1997.

Martin, N. and Monnier, J.: Adjoint accuracy for the full Stokes ice flow model: limits to the transmission of basal friction variability to the surface, The Cryosphere, 8, 721–741, 2014.

Milillo, P., Rignot, E., Rizzoli, P., Scheuchl, B., Mouginot, J., Bueso-Bello, J., and Prats-Iraola, P.: Heterogeneous retreat and ice melt of Thwaites Glacier, West Antarctica, Science advances, 5, eaau3433, 2019.

Morlighem, M., Rignot, E., Seroussi, H., Larour, E., Ben Dhia, H., and Aubry, D.: Spatial patterns of basal drag inferred using control methods from a full-Stokes and simpler models for Pine Island Glacier, West Antarctica, Geophysical Research Letters, 37, 2010.

Morlighem, M., Seroussi, H., Larour, E., and Rignot, E.: Inversion of basal friction in Antarctica using exact and incomplete adjoints of a higher-order model, Journal of Geophysical Research: Earth Surface, 118, 1746–1753, 2013.

Morlighem, M., Rignot, E., Binder, T., Blankenship, D., Drews, R., Eagles, G., Eisen, O., Ferraccioli, F., Forsberg, R., Fretwell, P., et al.: Deep glacial troughs and stabilizing ridges unveiled beneath the margins of the Antarctic ice sheet, Nature Geoscience, pp. 1–6, 2019.

Mosbeux, C., Gillet-Chaulet, F., and Gagliardini, O.: Comparison of adjoint and nudging methods to initialise ice sheet model basal conditions., Geoscientific Model Development, 9, 2016.

Mouginot, J., Rignot, E., and Scheuchl, B.: Sustained increase in ice discharge from the Amundsen Sea Embayment, West Antarctica, from 1973 to 2013, Geophysical Research Letters, 41, 1576–1584, 2014.

https://doi.org/10.5194/tc-2020-235
Preprint. Discussion started: 21 September 2020

National Academies of Sciences, Engineering, and Medicine: A Strategic vision for NSF investments in Antarctic and southern ocean research, National Academies Press, Washington, DC, 2015.

Pattyn, F., Favier, L., Sun, S., and Durand, G.: Progress in numerical modeling of Antarctic ice-sheet dynamics, Current climate change reports, 3, 174–184, 2017.

Pearson, K.: VII. Note on regression and inheritance in the case of two parents, proceedings of the royal society of London, 58, 240–242, 1895.

Perego, M., Price, S., and Stadler, G.: Optimal initial conditions for coupling ice sheet models to Earth system models, Journal of Geophysical Research: Earth Surface, 119, 1894–1917, 2014.

Petra, N., Zhu, H., Stadler, G., Hughes, T. J., and Ghattas, O.: An inexact Gauss-Newton method for inversion of basal sliding and rheology parameters in a nonlinear Stokes ice sheet model, Journal of Glaciology, 58, 889–903, 2012.

Raymond, M. J. and Gudmundsson, H.: Estimating basal properties of ice streams from surface measurements: a non-linear Bayesian inverse approach applied to synthetic data, The Cryosphere, 3, 265–278, 2009.

Rignot, E., Mouginot, J., Scheuchl, B., van den Broeke, M., van Wessem, M. J., and Morlighem, M.: Four decades of Antarctic Ice Sheet mass balance from 1979–2017, Proceedings of the National Academy of Sciences, 116, 1095–1103, 2019.

Scambos, T. A., Bell, R. E., Alley, R. B., Anandakrishnan, S., Bromwich, D., Brunt, K., Christianson, K., Creyts, T., Das, S., DeConto, R., et al.: How much, how fast?: A science review and outlook for research on the instability of Antarctica's Thwaites Glacier in the 21st century, Global and Planetary Change, 153, 16–34, 2017.

Seroussi, H., Morlighem, M., Larour, E., Rignot, E., and Khazendar, A.: Hydrostatic grounding line parameterization in ice sheet models, The Cryosphere, 8, 2075–2087, 2014.

Seroussi, H., Nowicki, S., Simon, E., Abe-Ouchi, A., Albrecht, T., Brondex, J., Cornford, S., Dumas, C., Gillet-Chaulet, F., Goelzer, H., Golledge, N. R., Gregory, J. M., Greve, R., Hoffman, M. J., Humbert, A., Huybrechts, P., Kleiner, T., Larour, E., Leguy, G., Lipscomb, W. H., Lowry, D., Mengel, M., Morlighem, M., Pattyn, F., Payne, A. J., Pollard, D., Price, S. F., Quiquet, A., Reerink, T. J., Reese, R., Rodehacke, C. B., Schlegel, N.-J., Shepherd, A., Sun, S., Sutter, J., Van Breedam, J., van de Wal, R. S. W., Winkelmann, R., and Zhang, T.: initMIP-Antarctica: an ice sheet model initialization experiment of ISMIP6, The Cryosphere, 13, 1441–1471, https://doi.org/10.5194/tc-13-1441-2019, https://www.the-cryosphere.net/13/1441/2019/, 2019.

Shepherd, A., Ivins, E., Rignot, E., Smith, B., Van Den Broeke, M., Velicogna, I., Whitehouse, P., Briggs, K., Joughin, I., Krinner, G., et al.: Mass balance of the Antarctic Ice Sheet from 1992 to 2017, Nature, 558, 219–222, 2018.

Sutterley, T. C., Velicogna, I., Rignot, E., Mouginot, J., Flament, T., Van Den Broeke, M. R., Van Wessem, J. M., and Reijmer, C. H.: Mass loss of the Amundsen Sea Embayment of West Antarctica from four independent techniques, Geophysical Research Letters, 41, 8421–8428, 2014.

Thorsteinsson, T., Raymond, C. F., Gudmundsson, G. H., Bindschadler, R. A., Vornberger, P., and Joughin, I.: Bed topography and lubrication inferred from surface measurements on fast-flowing ice streams, Journal of Glaciology, 49, 481–490, 2003.

Van Liefferinge, B. and Pattyn, F.: Using ice-flow models to evaluate potential sites of million year-old ice in Antarctica., Climate of the Past Discussions, 9, 2013.

Vieli, A. and Payne, A. J.: Application of control methods for modelling the flow of Pine Island Glacier, West Antarctica, Annals of Glaciology, 36, 197–204, 2003.

Weertman, J.: On the sliding of glaciers, Journal of glaciology, 3, 33–38, 1957.

https://doi.org/10.5194/tc-2020-235
Preprint. Discussion started: 21 September 2020

Yu, H., Rignot, E., Seroussi, H., and Morlighem, M.: Retreat of Thwaites Glacier, West Antarctica, over the next 100 years using various ice flow models, ice shelf melt scenarios and basal friction laws, The Cryosphere, 12, 3861–3876, 2018.

685 Zhao, C., Gladstone, R. M., Warner, R. C., King, M. A., Zwinger, T., and Morlighem, M.: Basal friction of Fleming Glacier, Antarctica–Part 1: Sensitivity of inversion to temperature and bedrock uncertainty, The Cryosphere, 12, 2637–2652, 2018.

Zhdanov, M. S.: Inverse theory and applications in geophysics, vol. 36, Elsevier, 2015.